Design History Files

Microfluidics Chip Design for

Liquid Phase and Solid Phase Synthesis

UBCV iGEM 2024

Written by: Jessica Xin

1.0 Needs Summary

1.1 Introduction

Microfluidics is a technology that involves the precise manipulation of fluids at the microscale. Through a set of interconnecting groves or microchannels engraved on a base chip, fluids are thoroughly mixed (Pattanayak et al., 2021). Due to its ability to handle small volumes of fluids with high precision and control, we can reduce reagent use and produce faster analysis times (Whitesides, 2006). The compact size allows precise control of physiochemical reactions of the fluid contained, with increased surface area resulting in high mass transfer and analytical throughput (Pattanayak et al., 2021).

In UBC iGEM's 2024 project on DNA data storage, we must assemble DNA rapidly and efficiently for synthesis. Thus, through designing a multitude of microfluidic chips, we hope to facilitate the precise delivery and mixing of nucleotides in controlled conditions (Battat et al., 2022). This allows the synthesis of long strands of DNA on a platform supportive of high-throughput synthesis through parallel production of multiple DNA sequences, making it scalable.

The Wet Lab Team's experimental plans consist of optimizing their thermostable-TDT-based nucleotide addition strategies in liquid phase (LPS), before implementing them at reduced volumes for solid phase synthesis (SPS). Given the high cost of reagents, the technical decision to implement a factorial design of experiments, and the high environmental impact of biohazardous plastic waste in such experiments - our UBCV iGEM team collectively decided to utilize microfluidic chips from the get-go.

1.2 Classifying Micromixers

Micromixers can be classified into Passive and Active based on their mixing mechanisms. In general, active micromixers require an external energy field to agitate fluids while passive micromixers rely on geometry and small size to manipulate the fluids (Wang et al., 2023). Table 1 summarizes the main differences between the two micromixers.

Table 1. Properties of active and passive micromixers (Wang et al., 2023).

Active	Passive
● Uses electric, thermal, magnetic, acoustic, and pressure fields to agitate fluid states ● Complex design ● Large in size ● Extensive power usage ● Very efficient at mixing and has few constraints on mixing conditions	● Uses special geometry structures to disturb flow states ● Simple design ● Small in size ● No energy consumption ● Requires stringent flow conditions for sub-par mixing

Given the context of iGEM's timeline, and taking into account our team's budget and capabilities, we chose to pursue multiple passive micromixer designs through DBTL cycles and evaluate their performance, rather than spend all our resources on one active mixer design.

1.3 Significance of Reynold's Number

The Reynolds number (Re) is a dimensionless quantity used in fluid mechanics to characterize the flow regime of a fluid within a flow channel. It is defined as the ratio of inertial forces to viscous forces and is given by this equation below:

$$Re = \frac{\rho v L}{\mu}$$

Where ρ is the fluid density, ν is the fluid velocity, L is the characteristic length of the flow channel, and μ is the dynamic viscosity of the fluid.

Reynolds number helps predict whether the flow will be laminar (smooth and orderly) or turbulent (chaotic and irregular). It is a value that provides a holistic representation of the fluid's behaviour, taking into account physical phenomena like shear stress, channel pressure and fluid resistance. In our designs, we should aim to replicate the Re values by the original authors when given. If not given, the formula should be derived using our workflow parameters so that the Re can be calculated. Ideally, our designs aim for a low Reynolds' number to ensure laminar flow; a higher Reynolds number would indicate more turbulent flow.

1.4 Identified Needs

Based on preliminary brainstorming and research, our team recognizes basic needs that our microfluidic chip designs must address for our project's purpose:

1. Minimizes use of reagents
2. Allow the trial of multiple concentrations
3. Easy to use with minimal training time
4. Scalable at low cost, allowing for parallel synthesis
5. Minimizes dead flow zones
6. Easy to fabricate with laser ablation
7. Reproducible as existing passive micromixer

2.0 Setting Requirements and Evaluation Criteria

2.1 Requirements

For usability and reproducibility, we produced design specifications for all microfluidic chips that are to be designed. These specifications are modified from Dr. Albert Folch's BIOEN 455 course at the University of Washington. It is important to follow these specifications to ensure the success of 3D printing and laser cutting the chips.

- Length of the chip has to be 50.00 mm
- Width of the chip has to be 60.00 mm
- There must be four holes in the corner of every layer, with a diameter of 5.00 mm
- Distance between the center of the four holes to the edge of the chip has to be 4.00 mm
- All inlet and outlet fluidic channel holes have to be 2.00 mm
- The distance between any inlet or outlet hole has to be greater than 10.00 mm
- Layers must be printed in 1mm thick acrylic PMMA plastic
- Sheets are to be bonded together by 3M 468MP Adhesive Transfer Tape

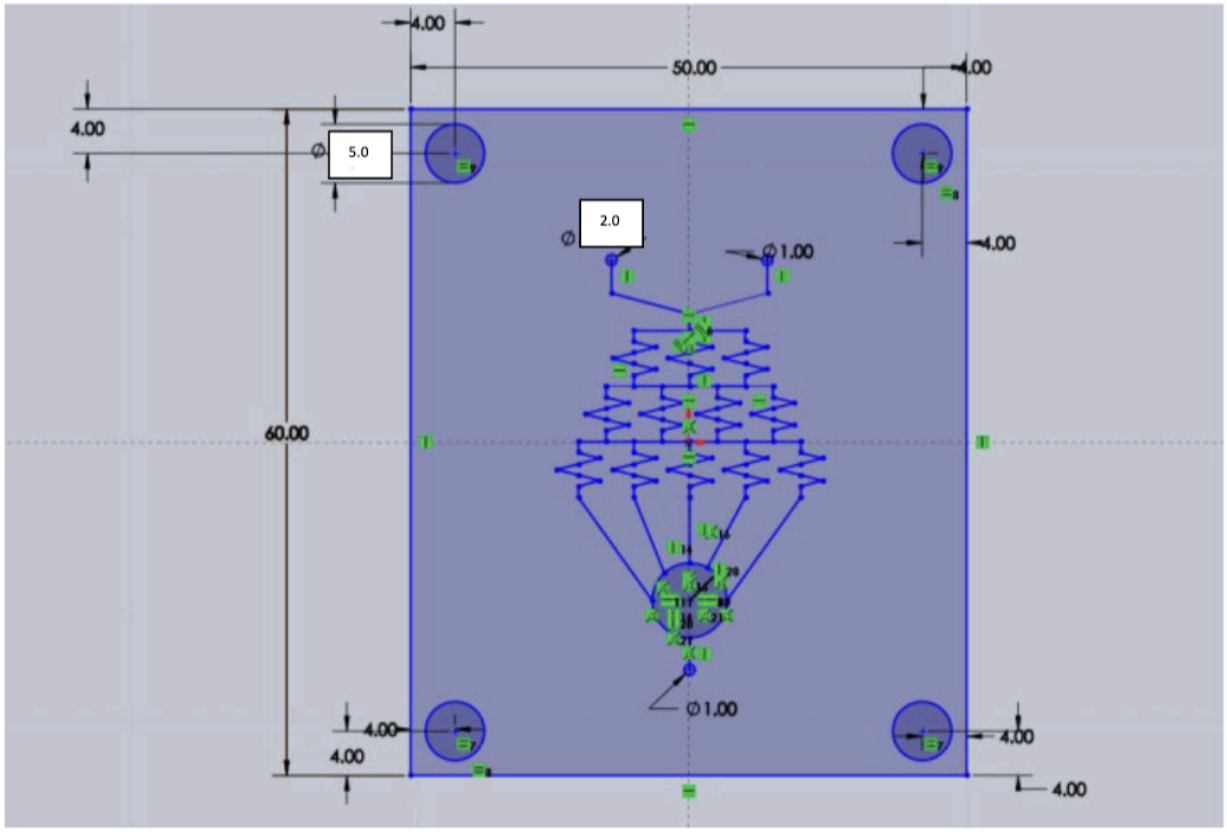

Figure 1. Design specifications for microfluidic chips.

More requirements that must be followed for the microfluidic chips are included in the table below, with correlations to our identified needs and justifications.

Table 2. Requirements for our microfluidic chip designs.

#	Requirement	Justification
1	The temperature used for flow simulations must be 37C.	This is to more accurately simulate the incubation conditions and to provide an optimal environment for DNA.
2	The face and base chips for each design must be the same.	To ensure reproducibility of inlet and outlet hole location and so that the nozzle and pumps work with all chips the same.
3	The fluid velocity used for flow simulations must be 0.000017 kg/s or less.	The most common speed at which researchers run their microfluidics pump is at 1 ml/min or less; our pumps will be running at this speed as well.
4	Assume that all input fluids behave like water.	Given that the reaction mix quantities (requirement #5) collectively represent an extremely small proportion of the total solution, we assume that the fluid behaves similarly to water in terms of density and viscosity. This helps simplify our Reynolds Number formula derivation and calculation.
5	Reaction mix for both solid and liquid phase synthesis consists of 10mM Potassium Acetate, 20mM Tris-Acetate, 10mM Magnesium Acetate.	For the above assumption to be true.
6	The time required to run the flow simulation should not take longer than 5 minutes.	The microfluidic chip designs are simple models such that simulations should not take long to run. To optimize computation power and usability in less powerful hardware, the mesh density should be adjusted such that the runtime should be less than 5 minutes.
7	The standard deviation of the mass fraction of liquid from the outlet must be less than 0.1.	From the flow simulation, we can determine the mass fraction of input liquid at a large number of points at the output channel. The standard deviation can then be calculated and the closer it is to 0, the more the fluid is mixed. The mass fraction should be 0.5 for perfect mixing at the outlet channel; to ensure that the design is properly mixing, the standard deviation for the mass fraction values should be as close to 0 as possible.
8	The same guide plate should be used in each	To ensure layers are assembled the same way, on the same rods, between each design for better success at 3D printing

	design to assemble the layers.	
9	Chips designed for liquid phase synthesis should have at least 3 layers.	Microfluidic devices can range from 2 to 20 layers depending on their functionality (Chambers, 2021). For LPS, two of the layers should consist of the base and face chip. The face chip is to ensure liquid doesn't overflow as it flows through the channels. The layers in between will consist of special geometry that differs between each design. Thus, each design should at least have 3 layers in total.
10	Chips designed for solid phase synthesis should have at least 2 layers.	Same justification as above. For solid phase synthesis, the face plate is not required since the molecules are synthesizing on a solid material.
11	Each microfluidic chip should have less than 8 layers.	In consideration of sustainability and complexity, our microfluidic chips are all passive micromixers, which are smaller in size and simpler in design. The most common designs are easily encompassed in three layers or less.
12	The assembled chips must not leak.	When physically testing the chips, the chips must not leak to ensure that reagents and molecules are not lost when inputted into the channels as we are handling DNA.

2.2 Evaluation Criteria

1. *Standard Deviation of Mass Fraction of Water at Output*

This is the metric that we will be using to evaluate our designs in Solidworks Flow Simulation. The closer the standard deviation is to 0, the greater the satisfaction as the fluid is mixed more fully closer to 0. This is a linear relationship as satisfaction levels decrease the same when there is an increase in standard deviation.

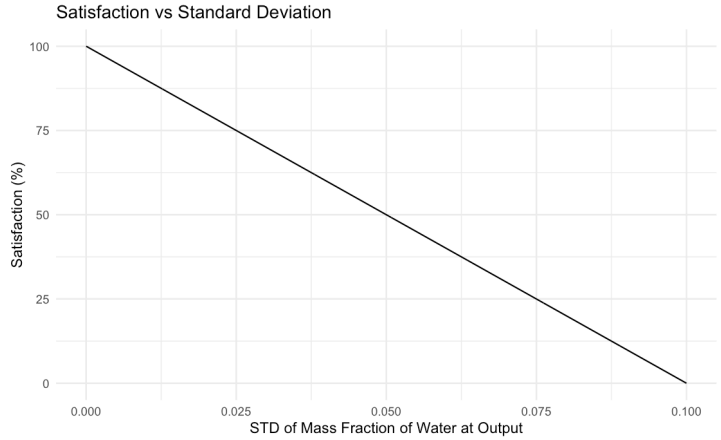

Figure 2. Satisfaction curve for evaluation criteria #1.

2. *Time required to run flow simulations*

Our virtual method of testing will be through Solidworks Flow Simulations. The runtime would therefore be directly proportional to how easy and quickly the mixing and experiment will occur in the lab. A piecewise optimum curve was used to take into consideration the accuracy of our simulation model. The mesh density must be decreased for a very fast runtime, which would decrease the accuracy of the analysis results. Thus, to optimize both accuracy and runtime, max satisfaction would occur at 1.5 minutes, the standard time required to run a microfluidic chip flow simulation at a medium-mesh density of 4.

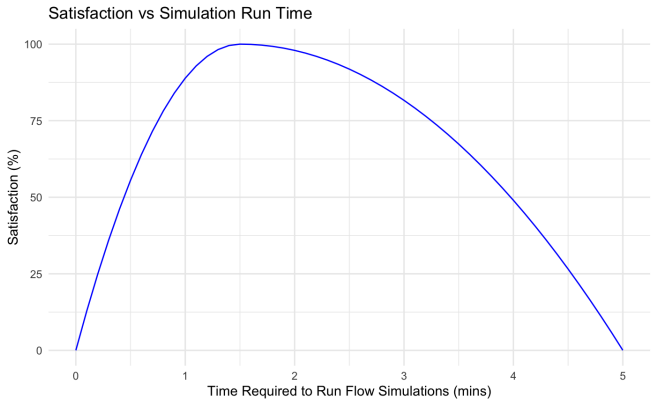

Figure 3. Satisfaction curve for evaluation criteria #2.

3. *Color Intensity of Titration Experiments*

Our physical method of testing the laser printed chips will be through a simple titration experiment (see Section 4 for a description of this test). The green value at the outlet of each LPS chip design was measured and compared against a neutralized green color of the bromothymol blue indicator. A piecewise optimum curve was used as anything above the neutralized green color is considered too yellow / too acidic and anything below is considered too blue / too basic. The minimum values were obtained from the most basic blue color and the most acidic yellow color. Anything above or below the neutralized green value would lower the satisfaction.

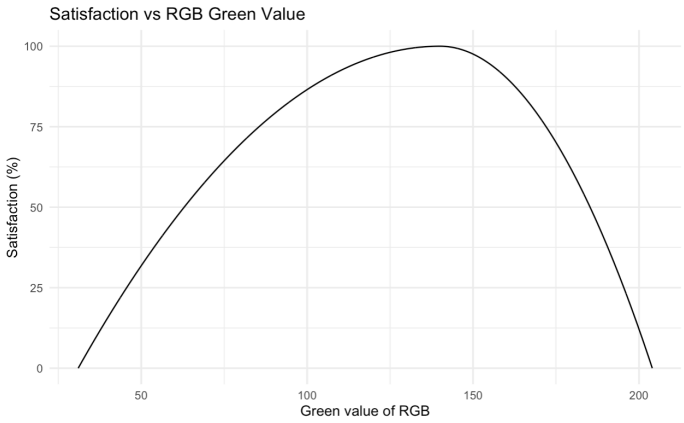

Figure 4. Satisfaction curve for evaluation criteria #3.

4. *Plastic Waste*

While implementing microfluidic chips in our workflow encourages a more sustainable use of reagents and reactions, we need to ensure the manufacturing process is as sustainable as possible. Some designs have differing complexity and differing amounts of layers. Each layer is made out of PMMA plastic, thus, to evaluate our plastic use, satisfaction decreases with more plastic layers. It is discrete since layers are either 3, 4, 5, or 6. Maximum satisfaction is at 3 layers since all designs have the same base and face chip, with a minimum of one specially designed chip in between.

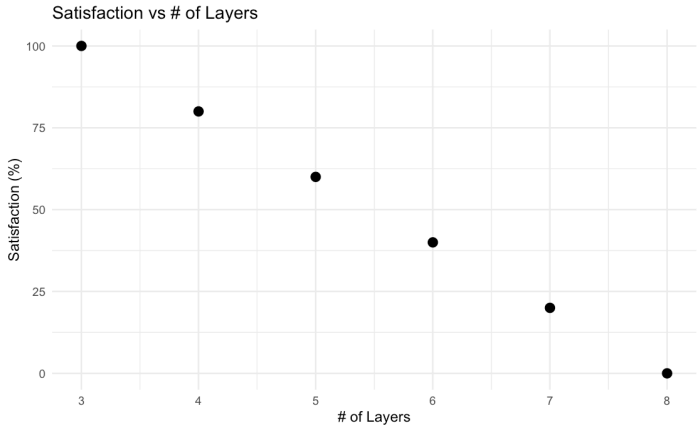

Figure 5. Satisfaction curve for evaluation criteria #4.

5. *Assembly Complexity*

Following the laser ablation of each chip, plastic bits must be manually removed and each layer has to be assembled. Depending on the intricacy and complexity of the channel design, some layers may require a microscope to carefully remove microscopic bits of plastic. The placement of adhesive may also affect how easy it is to assemble each layer. Based on these factors, the difficulty in assembling each design can differ. Thus, individuals that contributed to assembling each chip are asked to quantitatively determine the difficulty on a scale. More satisfaction is associated with decreased difficulty, thus, a decreasing linear plot is used.

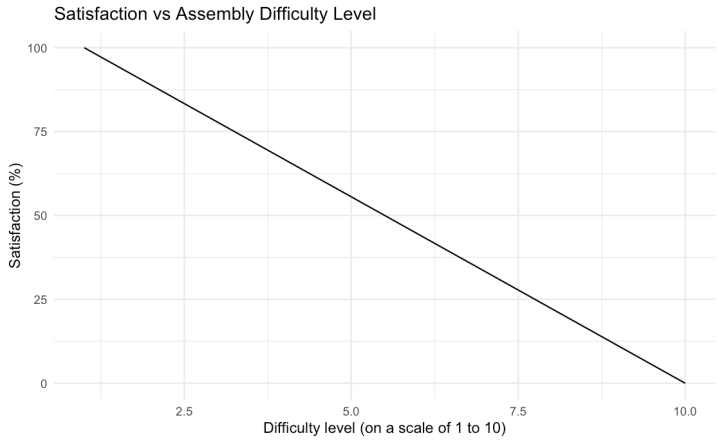

Figure 6. Satisfaction curve for evaluation criteria #5.

3.0 Concept Generation + Prototyping

3.1 Literature Review of Passive Micromixer Designs

Through a comprehensive review of Wang et al.'s (2023) overview of the most current and relevant passive micromixers designs, each category is summarized below based on Figure 7.

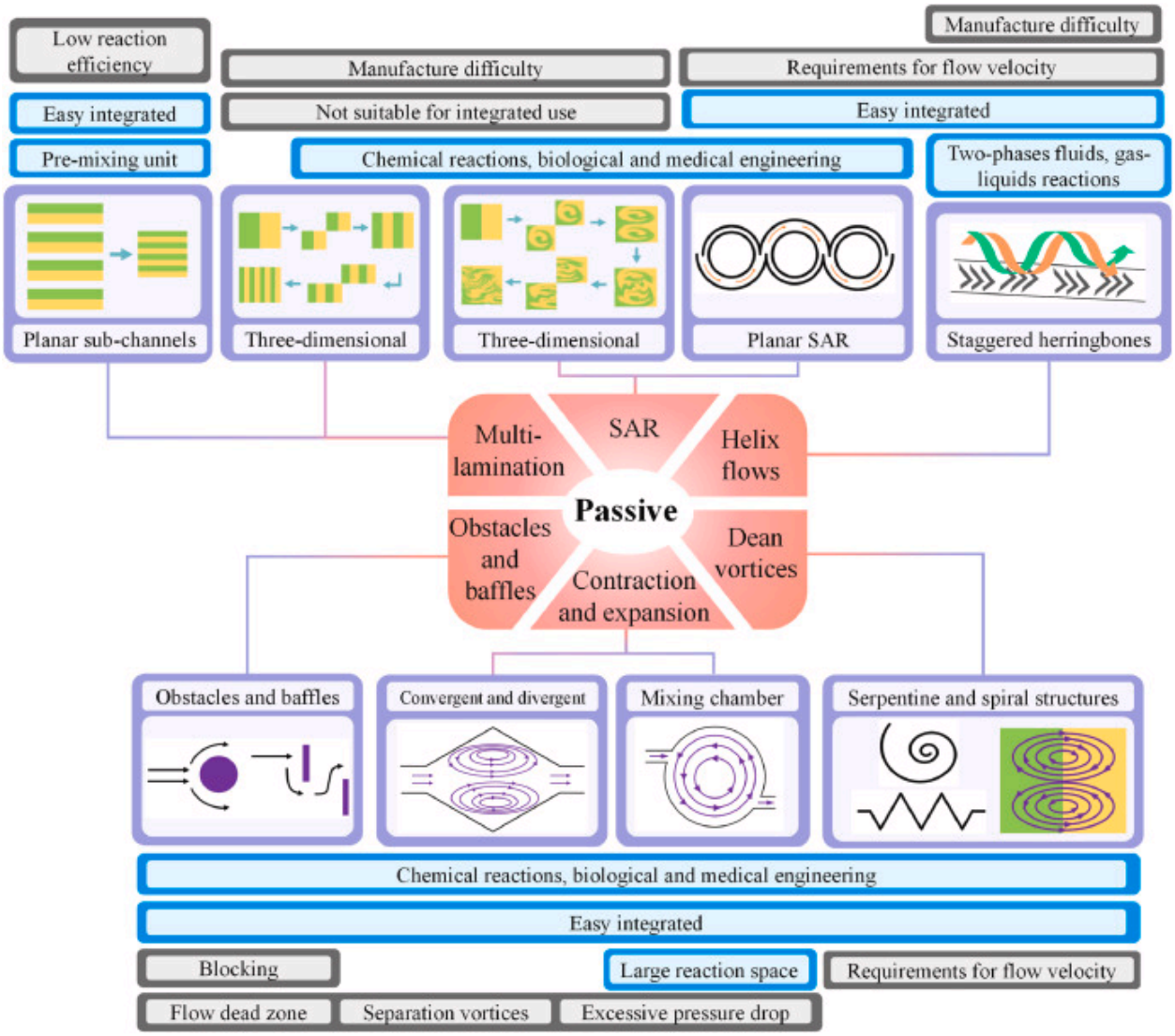

Figure 7. Image from Wang et al.'s (2023) paper showing the six classifications of passive micromixers.

Multilamination Effects

The multi-lamination effect relies on splitting the fluid stream into multiple smaller streams which are then recombined, increasing the interfacial area to shorten diffusion distance in laminar flow states. Molecular diffusion is one of the primary mixing mechanisms at the microscale, especially in laminar flow conditions. Multilamination effects are more effective in

three-dimensional subchannels than planar ones in obtaining a more efficient uniform mixing. Planar subchannels are useful for integrated and pre-mixing uses.

Splitting and Recombining Structures (SAR)

SAR-based designs mix fluids by dividing the main inlet stream into two or more subchannels and then recombining them. In contrast to multilmaniation effects, the main mixing process of SAR structures is chaotic advection since the interfacial area between different fluid streams is increased, causing the interface between streams to become distorted. Traditional SAR structures contain asymmetric circular or rhombic subchannels to induce Dean vortices for effective fluid mixing. Three-dimensional SAR structures also had better mixing performance than planar ones as fluid collisions can occur in multiple directions, further increasing interfacial area.

Baffles and Obstacles

Baffles and obstacles induce mixing by directly changing flow direction and producing transverse flows. Changes in flow direction cause the fluid to fold and stretch continuously, while the transverse flows create separation vortices and flow dead zones that inhibit substance transport. Thus, these are often used as secondary structures to strengthen chaotic advection and improve mixing in passive micromixers. However, the flow dead zones and separation vortices may cause increased pressure drops and hinder substance transport.

Contraction and Expansion Effects (CAE)

CAE designs utilize variations in channel cross-sections to enhance fluid mixing through the generation of vortices and flow velocity changes. It leverages reverse pressure gradients that form when fluid flows from a narrow channel into a wider one, creating expansion vortices. These vortices disrupt the flow and promote chaotic advection, creating eddy currents that increase the mixing of fluids. CAE structures are easy to construct and are more effective in three-dimensional than planar. A potential drawback would be the formation of flow dead zones due to the separation of expansion vortices from the main streams. This can be mitigated by ensuring a high enough fluid velocity within the channels to maintain flow in all regions.

Helix Flows

Helix flow structures induce chaotic flows through staggered herringbones or grooves, making it easy to integrate with other micromixer structures. The helical structures induce rotational flow components, increasing the interaction between fluid layers and promoting efficient mixing within a compact device footprint. This design is particularly effective in achieving rapid and thorough mixing, making it ideal for various lab-on-a-chip applications. There is no risk of flow dead zones or pressure drops.

Dean Vortices

Dean vortices cause chaotic advection mixing, typically constructed of serpentine and spiral microchannels. When fluids flow in a curved microchannel, central fluids flow faster than the peripheral fluids, causing the outside fluids to be pushed to the top and bottom, generating counter-rotating vortices. These structures have no risk of flow dead zones and are easy to manufacture.

3.2 Reynolds' Number Calculation

First, to find the fluid velocity parameter, we used the Continuity Equation from fluid dynamics. The Continuity equation is rooted in the law of conservation of mass, and states that mass cannot be created or destroyed in a closed system. Thus, assuming an incompressible fluid:

$$Q = A \times v$$
$$v = \frac{Q}{ab}$$

where:

- Q is the volumetric flow rate
- $A = ab$ is the cross-sectional area (a rectangular duct with width b and height a) through which the fluid flows
- v is the fluid velocity

Next, to find the characteristic linear dimension, we assume the microfluidic channels act as square ducts, where L would correspond to the hydraulic (wetted surface) diameter of the channel. Given a square duct with width b and height a:

$$L = \frac{4ab}{2(a+b)} = \frac{2ab}{a+b}$$

Using the L and v we derived, the equation is updated to:

$$Re = \frac{\rho v L}{\mu} = \frac{\rho Q L}{\mu ab} = \frac{\rho Q 2ab}{\mu(a+b)ab} = \frac{2\rho Q}{\mu(a+b)} \quad (1)$$

As per our requirement, we assume that the fluid behaves like water. Parameters like the density (ρ) and dynamic viscosity (μ) can be obtained from the standard values for water at room temperature. Furthermore, since we are using laser ablation to cut the channels in sheets of PMMA plastic, the height of the rectangular channels (a) are assumed to be fixed at the thickness of the sheets. The volumetric flow rate (Q) is 1 $\frac{ml}{min}$, the speed at which our pumps are outputting at. The parameter values would be: $\rho = 1000\frac{kg}{m^3}$, $\mu = 0.001\frac{kg}{ms}$, $a = 0.0011m$.

Rearranging equation (1) and assuming we know the Re value would leave with only one unknown (b):

$$b = \frac{2\rho Q}{\mu Re} - a$$

Plugging in our known values, we have a working formula used to calculate the width of our channels (b):

$$b = \frac{2 \times 1000 \frac{kg}{m^3} \times 1.7 \times 10^{-8} \frac{m^3}{s}}{0.001 \frac{kg}{ms} \times Re} - 0.011m$$

$$b = \frac{0.034}{Re} m - 0.011m$$

3.3 Solidworks CAD Designs

We attempted to encapsulate all six passive micromixer designs over our LPS and SPS chips.

LPS Design 1 - Herringbone (Helix Flows)

For the Helix Flows design, we referenced Channon et al's (2021) design of a self-pumping microfluidic staggered herringbone mixer.

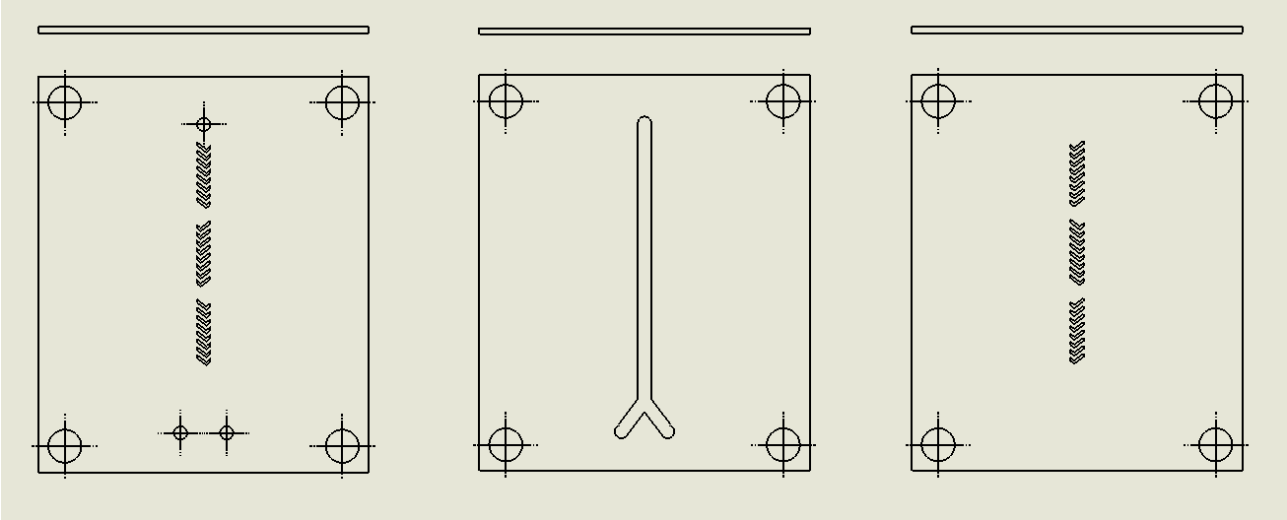

Figure 8. Herringbone Design.

LPS Design 2 - Countered Spirals (Dean Vortices)

For the Dean Vortices design, we referenced Hong & Yeom's (2022) design of a 3D serpentine channel. The paper simulated the design under different Reynolds numbers and showed the mixing index as a function of distance along the channel for the different values.

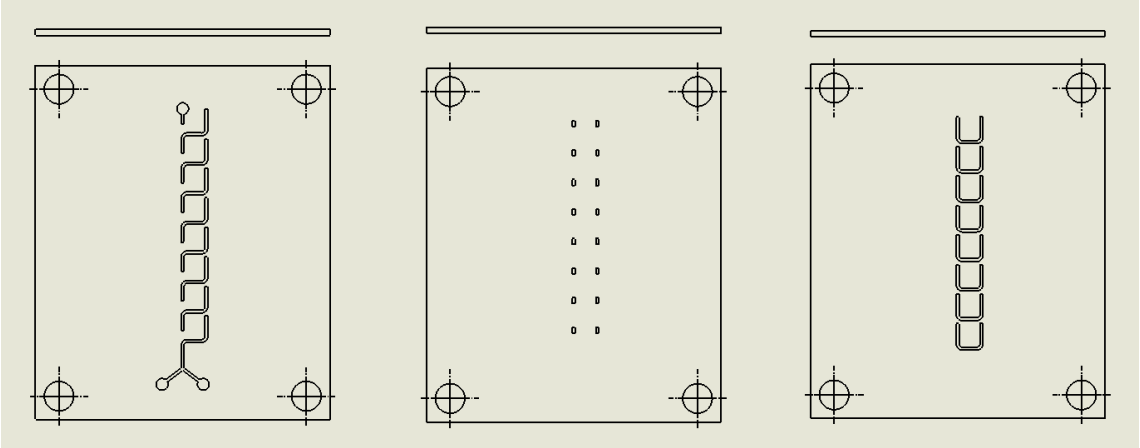

Figure 9. Dean Vortices Countered Spirals Design.

LPS Design 3 - 3D SAR

For the SAR design, we referenced Xia et al's (2005) design of a two-layer crossing channel at a low Reynolds number for fast mixing.

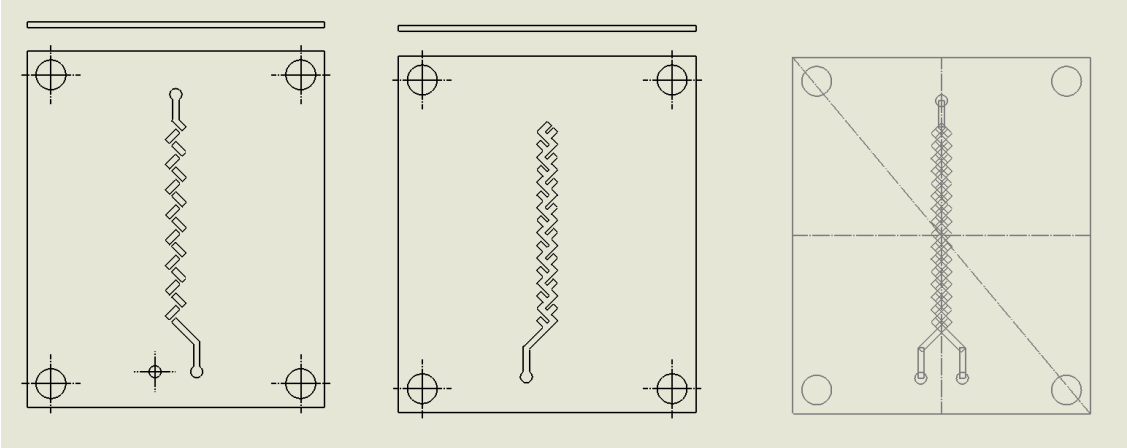

Figure 10. 3D SAR design.

LPS Design 4 - 3D SAR (F-channels)

For the F-channels design, we referenced Kim et al's (2005) design of a serpentine laminating micromixer that combined SAR and advection.

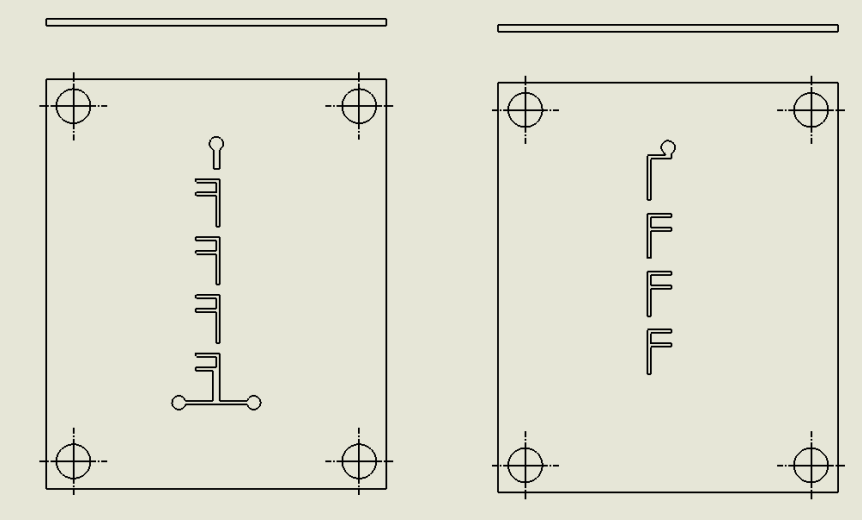

Figure 11. F-Channels design.

LPS Design 5 - 3D Multi Lamination

For the Multi Lamination design, we referenced Suh & Kang's (2010) paper.

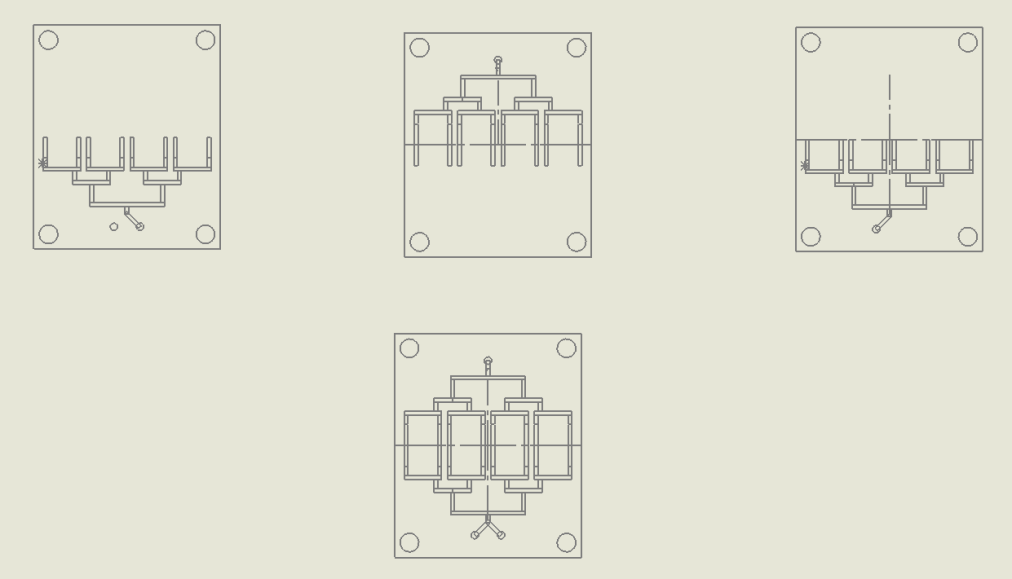

Figure 12. Multi Lamination design.

LPS Design 6 - CAE

For the CAE design, we referenced Viktorov et al's (2016) design of a chain micromixer.

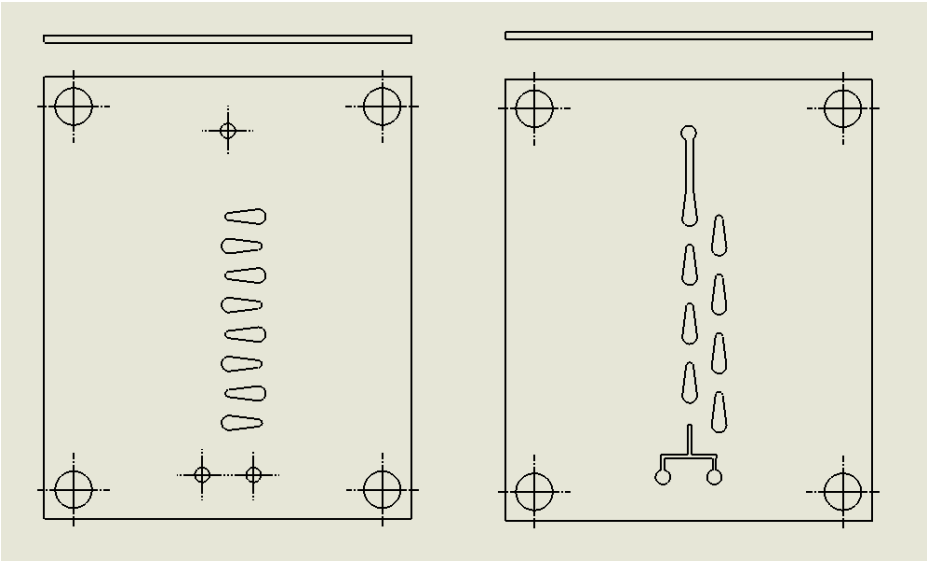

Figure 13. CAE design.

SPS Design 1 - Fin Shaped Baffles

For the Fin Shaped Baffles design, we referenced Cortes-Quiroz et al's (2010) design of a planar micromixer with fin shaped baffles for a wide Reynolds number flow range.

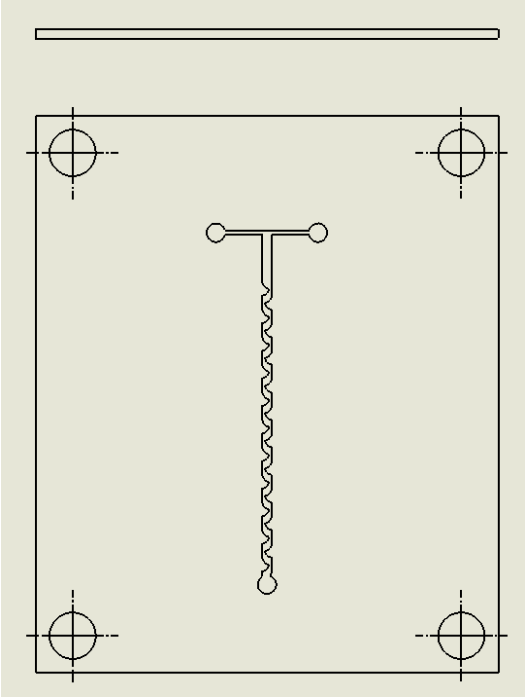

Figure 14. CAE design.

SPS Design 2 - Serpentine (Dean Vortices)

For the dean vortices design, we referenced Yin et al's (2021) design of a micromixer with mathematical spiral structures.

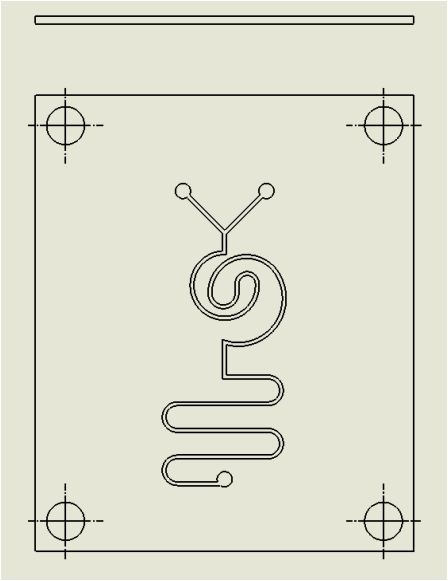

Figure 15. Serpentine design.

SPS Design 3 - CAE ZigZag

For the CAE ZigZag design, we referenced Natsuhara et al.'s (2022) design of a planar asymmetric CAE micromixer.

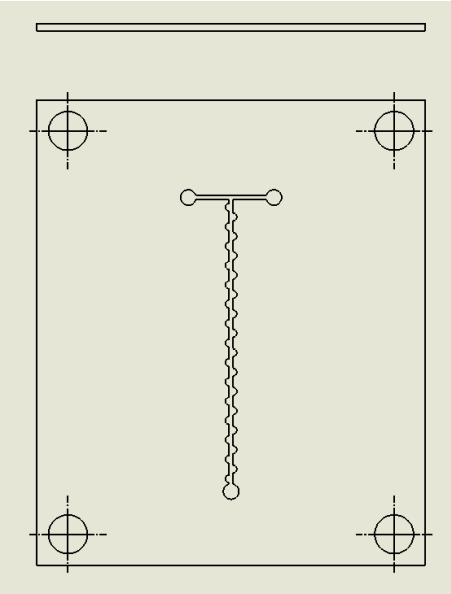

Figure 16. CAE ZigZag design.

SPS Design 4 - Planar SAR

For the Planar SAR design, we referenced Husain et al.'s (2018) design of an SAR micromixer with offset inlets.

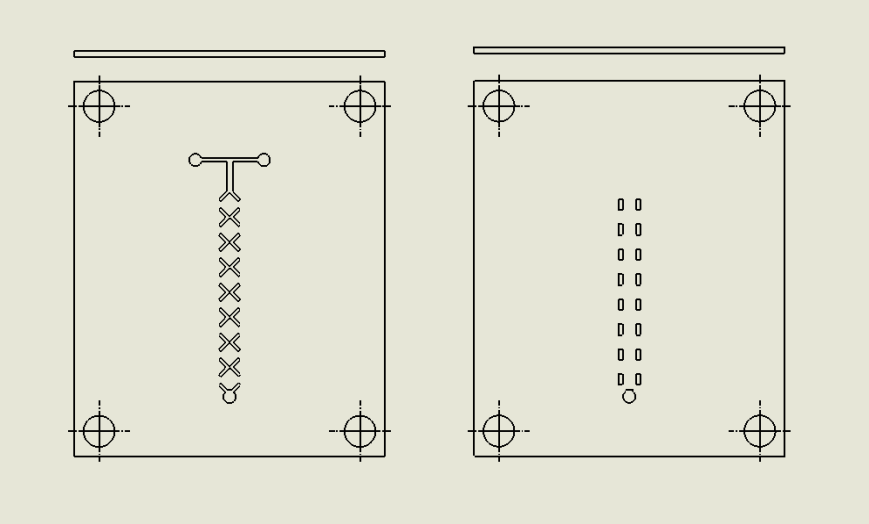

Figure 17. Planar SAR design.

SPS Design 5 - Cantor Baffles

For this design, we referenced Wu & Chen's (2019) design of a rectangular fractal micromixer, the imitate Cantor structure (ICS).

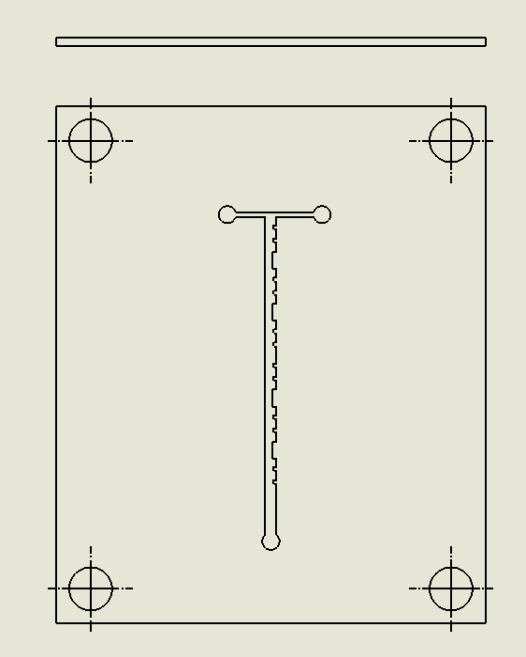

Figure 18. Cantor Baffles design.

3.4 Preliminary Concept Elimination

All designs are well-researched passive micromixers that meet all our requirements and needs. All designs met the chip specifications and used the same face, base, and guide plates for assembly. We plan to simulate all designs, perform a titration mixing experiment, and then score them based on our evaluation criteria to determine the most efficient design to provide to our Wet lab team.

4.0 Simulations, Testing, and Scoring

4.1 Solidworks Fluid Simulation Introduction

Through Solidworks Fluid Simulation tools, we can undergo computational fluid dynamics testing on our microfluidic chip designs. Computational fluid dynamics (CFD) is the science of using computers to predict liquid and gas flows based on the governing equations of conservation of mass, momentum, and energy (Ansys, n.d.). The fluid flow domain is represented by a CAD model, a mesh is then applied to dissect the domain into well-defined cells. Finally, the discretized version of the governing fluid equations is solved by the computer within each cell; this process is then repeated incrementally. Virtual simulations were preferred over physical mixing experiments since they can produce easily understandable results and animations that are postable on the iGEM wiki. Furthermore, we can easily calculate the mixing matrix for the scoring of each design.

4.2 Simulation Protocol

Setting the parameters on temperature, input liquid, mass flow rates, and mesh density will greatly influence the simulation results. To accurately model our in-lab conditions, these parameters and conditions were set for each simulation:

1. Liquid type for both inlet channels are assumed to be water
2. Analysis type: External
3. Initial concentration in system: 50% of liquid 1, 50% of liquid 2
4. Inlet Channels (type = flow opening, inlet profile = uniform)
    a. Inlet #1
        i. Mass fraction of liquid 1: 1
        ii. Mass fraction of liquid 2: 0
        iii. Mass flow rate: 0.000017 kg/s (matching 1 ml/min)
    b. Inlet #2
        i. Mass fraction of liquid 1: 0
        ii. Mass fraction of liquid 2: 1
        iii. Mass flow rate: 0.000017 kg/s (matching 1 ml/min)
5. Outlet Channel (type = pressure opening)
    a. Environment pressure
6. Temperature: 37℃ (310.15 K)
7. Mesh Density: 4

Once the simulation is run and results are calculated, we can then see the flow trajectory and select point parameters to analyze the mass fraction of water at the outlet channel. Intuitively, the outlet channel should be the point at which the fluids should be maximally mixed. Previously, methods for quantifying mixing between two or more coloured liquids involved a measure of standard deviation through mixing indices (Hashmi & Xu, 2014). Thus, we want to

communicate the spread of concentrations that are present at our outlet valve, which would also involve calculating the standard deviation of the mass fraction. The point parameters function provides the mass fraction at 100 points (can be altered) on the outlet channel. The values were then exported into excel to calculate the standard deviation. This measure will tend to 0 as the fluid is mixed more fully.

4.3 Simulation Results

The standard deviation values obtained from each design is summarized in Figure below. For the LPS chips, the F-Channels design outputted the lowest standard deviation, indicating it was the most efficient at mixing based on the simulation. Similarly, the best mixing SPS chip was the Fin-Shaped Baffles.

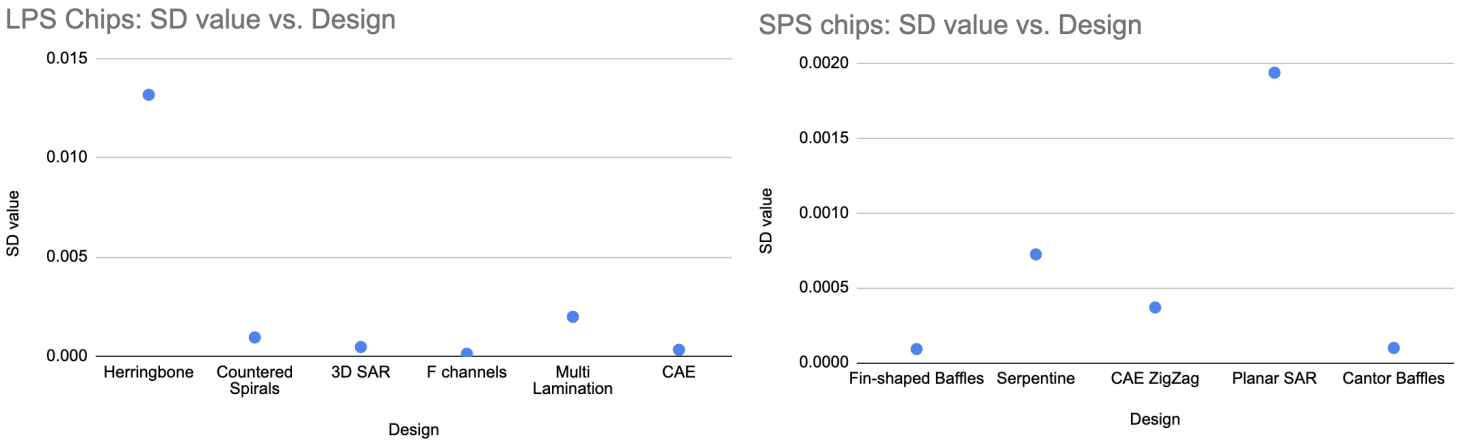

Figure 19. Plots indicating the standard deviation value of each chip design.

Training Chip

For training purposes, we constructed a training chip with no special geometry in place. As a control, we also simulated the training chip to show that our other micromixer designs should provide better mixing and a standard deviation closer to 0. A standard deviation of 0.1171 was obtained over 139 iterations and a runtime of 2.5 minutes.

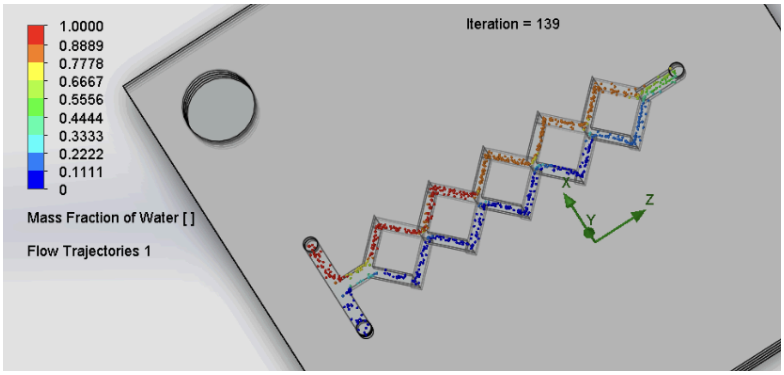

Figure 20. Flow trajectory of the training chip

LPS Design 1 - Herringbone (Helix Flows)

A standard deviation of 0.01316 was obtained over 113 iterations and a runtime of 1.75 minutes.

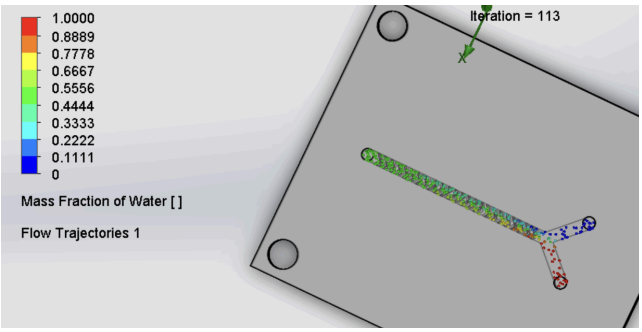

Figure 21. Flow trajectory of the herringbone design

LPS Design 2 - Countered Spirals (Dean Vortices)

A standard deviation of 0.00009505 was obtained over 234 iterations and a runtime of 2 minutes.

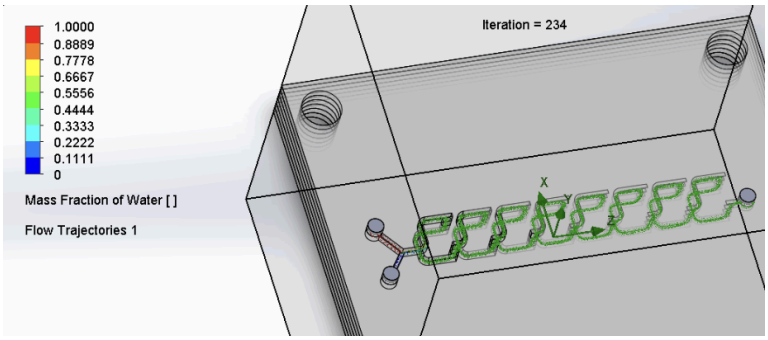

Figure 22. Flow trajectory of the dean vortices design.

LPS Design 3 - 3D SAR

A standard deviation of 0.0004678 was obtained over 145 iterations and a runtime of 2 minutes.

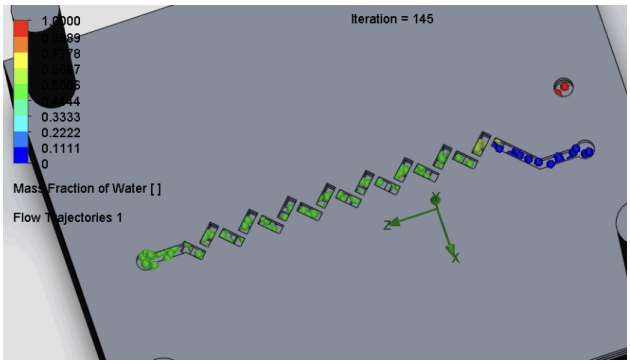

Figure 23. Flow trajectory of the 3D SAR design.

LPS Design 4 - 3D SAR (F-Channels)

A standard deviation of 0.0001285 was obtained over 95 iterations and a runtime of 1 minute and 20 seconds.

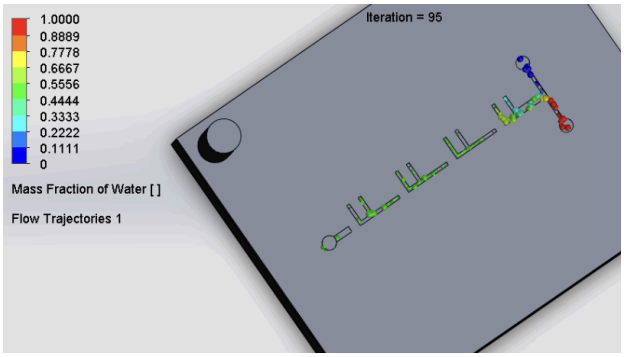

Figure 24. Flow trajectory of the 3D SAR, F-Channels design.

LPS Design 5 - 3D Multi Lamination

A standard deviation of 0.001987 was obtained over 147 iterations and a runtime of 3 minutes. From the simulations alone, we see that the liquid does not flow through all channels, indicating a dead zone at the first channel split.

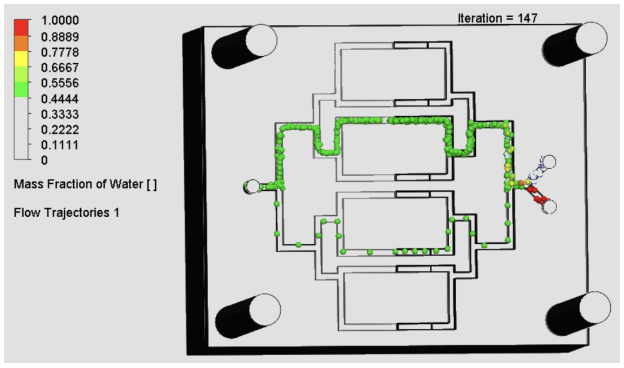

Figure 25. Flow Trajectory of the Multi Lamination Design.

LPS Design 6 - CAE

A standard deviation of 0.0003301 was obtained over 158 iterations and a runtime of 3 minutes.

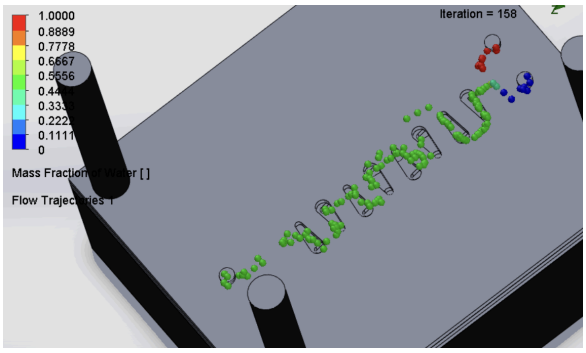

Figure 26. Flow Trajectory of the CAE Design.

SPS Design 1 - Fin Shaped Baffles

A standard deviation of 0.00009107 was obtained over 96 iterations and 2 minute runtime.

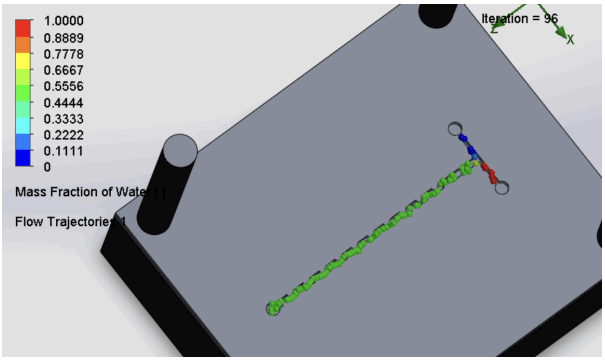

Figure 27. Flow Trajectory of the Fin-Shaped Baffles Design.

SPS Design 2 - Serpentine (Dean Vortices)

A standard deviation of 0.0007230 was obtained over 182 iterations and a runtime of 2 minutes and 30 seconds.

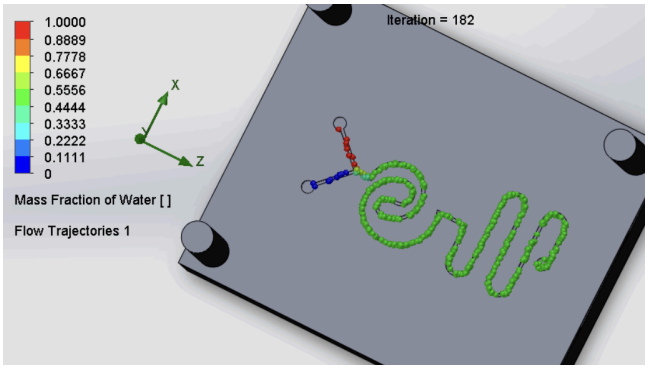

Figure 28. Flow Trajectory of the Serpentine Design.

SPS Design 3 - CAE ZigZag

A standard deviation of 0.0003687 was obtained over 123 iterations and a 2 minute runtime.

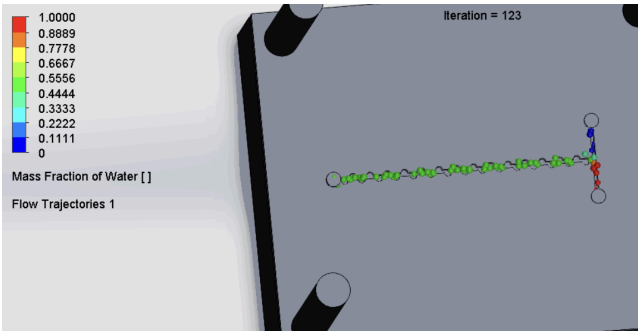

Figure 29. Flow Trajectory of the CAE ZigZag Design.

SPS Design 4 - Planar SAR

A standard deviation of 0.001935 was obtained over 97 iterations and a runtime of 2 minutes.

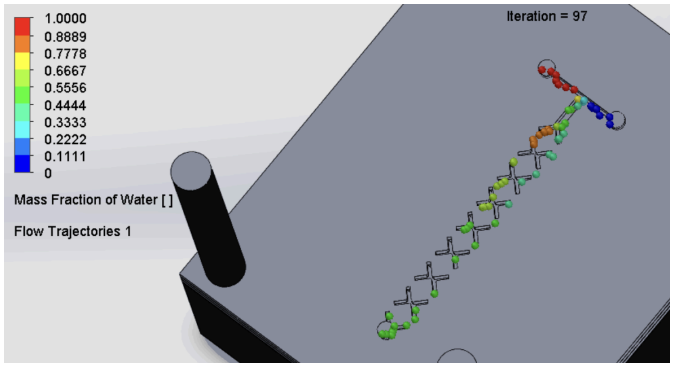

Figure 30. Flow Trajectory of the Planar SAR Design.

SPS Design 5 - Cantor Baffles

A standard deviation of 0.00009860 was obtained over 101 iterations and a runtime of 1 minute and 30 seconds.

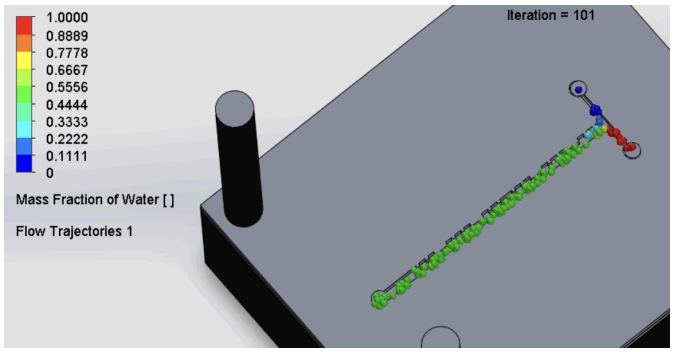

Figure 31. Trajectory of the Cantor Baffles Design.

The simulation results helped evaluate our designs against criterion 1 and 2, with which are plotted on our satisfaction curves in the figures below for LPS and SPS designs.

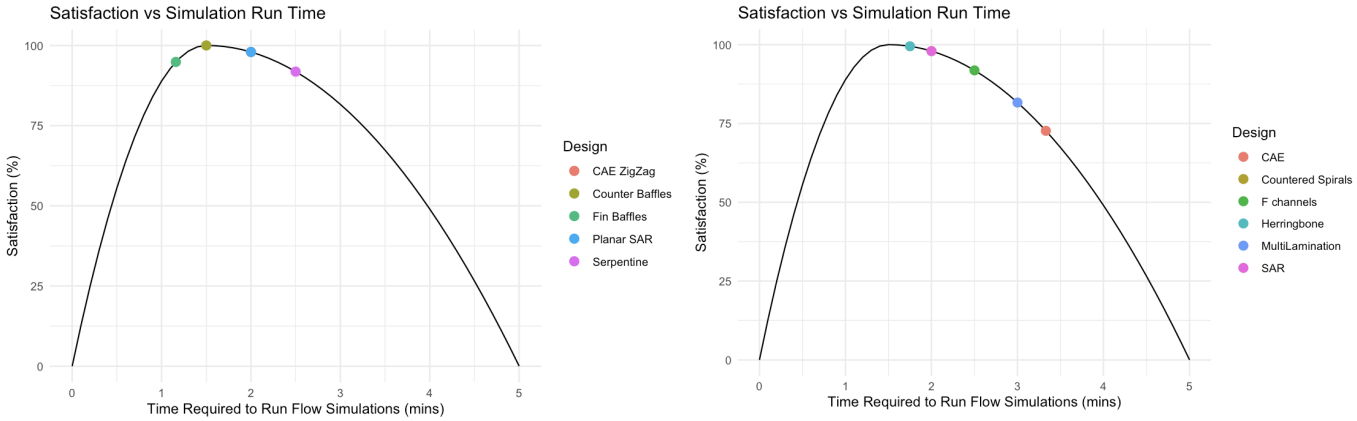

Figure 32. LPS (left) and SPS (right) satisfaction curves for simulation run time.

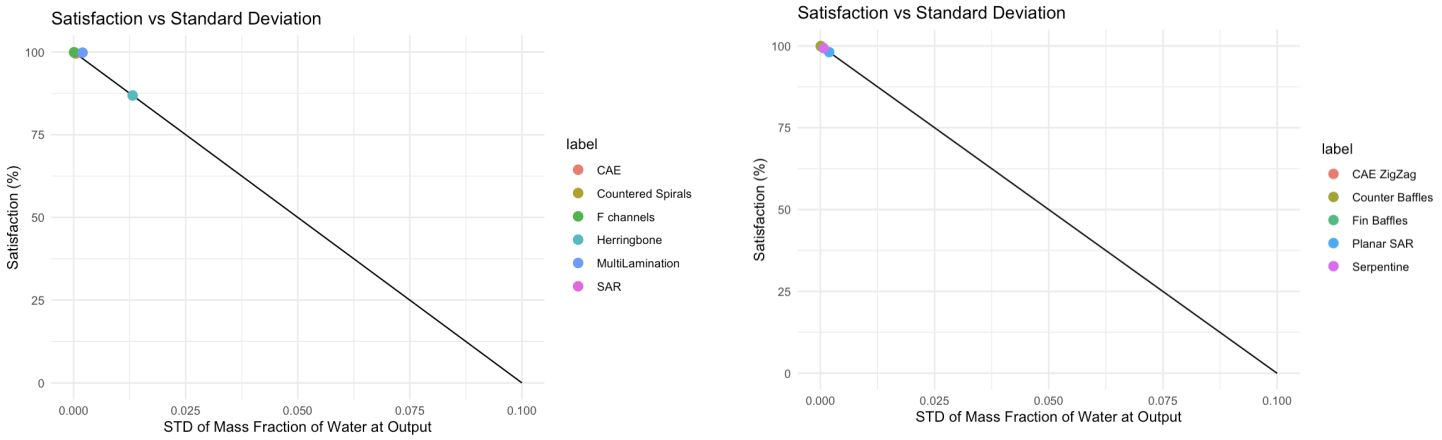

Figure 33. LPS (left) and SPS (right) satisfaction curves for standard deviation.

4.4 Plastic Waste and Assembly Testing

As per our evaluation criteria, we evaluated the plastic usage of each of our chip designs by counting how many layers they require. Similarly, the difficulty level of assembling each chip was assessed as per that evaluation criteria, with the satisfaction curves produced below.

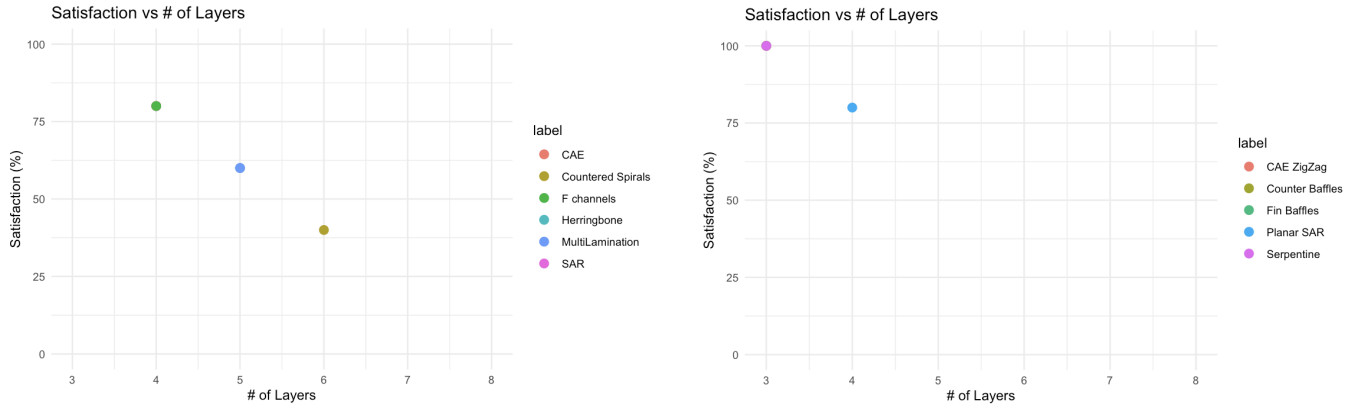

Figure 34. LPS (left) and SPS (right) satisfaction curves for # of layers.

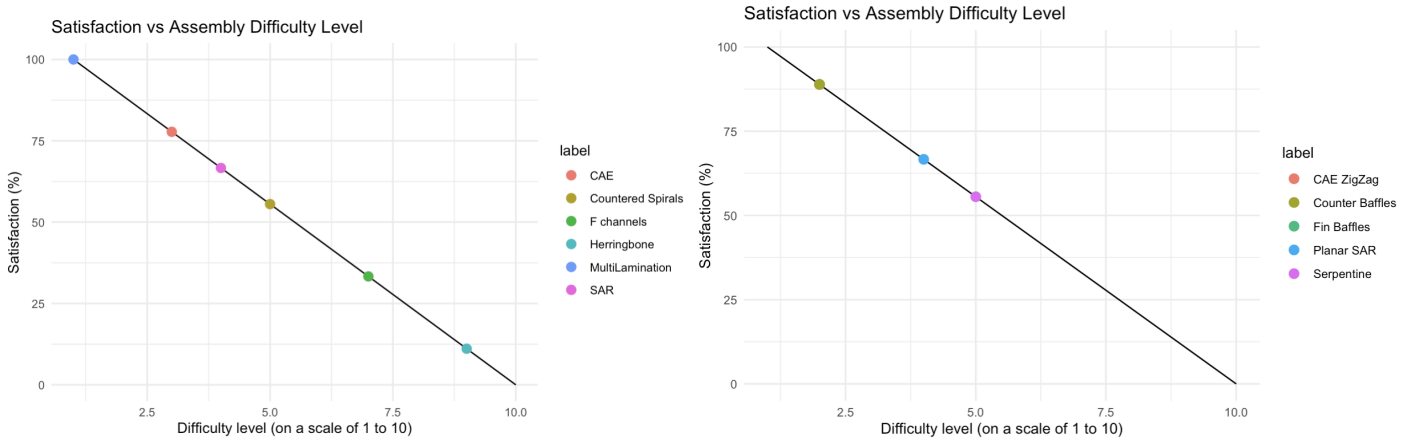

Figure 35. LPS (left) and SPS (right) satisfaction curves for assembly difficulty.

4.5 Titration Experiment Testing

To physically test our LPS microfluidic chip designs' mixing efficiency, we performed a simple titration experiment. We created two syringe pumps, which would pump NaOH through one inlet and HCl through another inlet. The base and acid would have an indicator, bromothymol blue added to them, which would indicate blue for base and yellow for acid. Refer to Figure 36 for the color and its relative pH level. As the strong base and acid mixes throughout the chip channels, it would neutralize to green color at the outlet channel. Using a digital color meter, the hexadecimal # and RGB values of the color of the liquid at the outlet channel were measured and the results are included in table 3. The RGB values of the neutralized green, most basic blue, and most acidic yellow were used as references to compare against to produce the satisfaction curve in Figure 37.

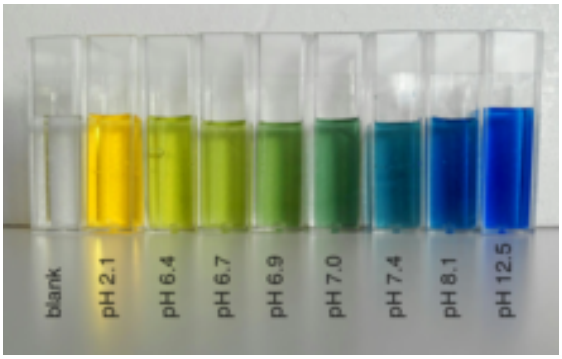

Figure 36. pH and color ranges for the bromothymol blue indicator. A pH of 6.9 had a green value of 140, a pH of 12.5 had a green value of 31, and a pH of 2.1 had a green value of 204; these values were used as references.

Table 3. Neutralization Color Measurement Results.

LPS Design	Hexadecimal #	Green Value
Herringbone	#aaa77a 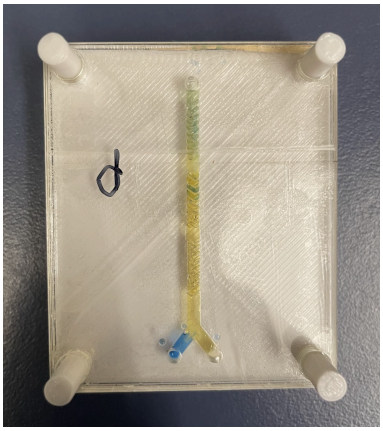	167

Countered Spirals	#c8cc8f 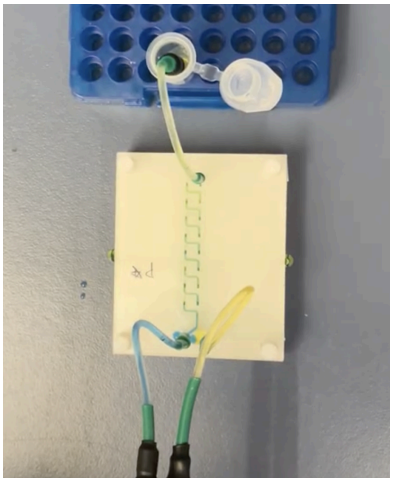	204
SAR	#a6b096 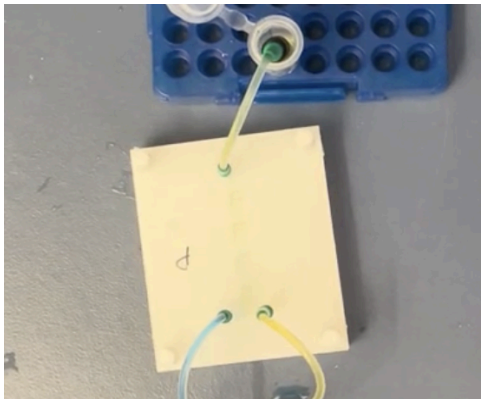	176
CAE	#a6b190 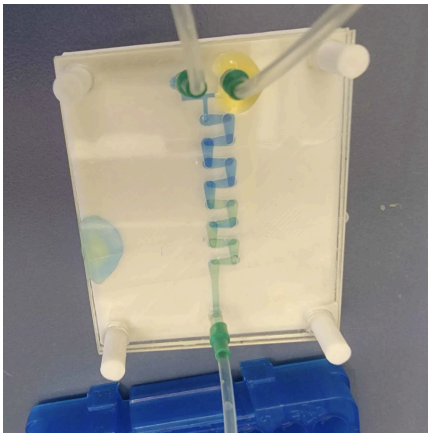	177

F Channels	#cccf9e 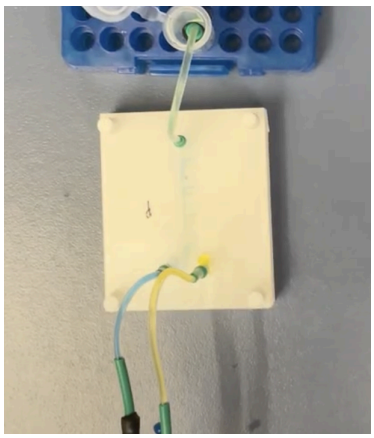	200
Multi Lamination	#b9be81 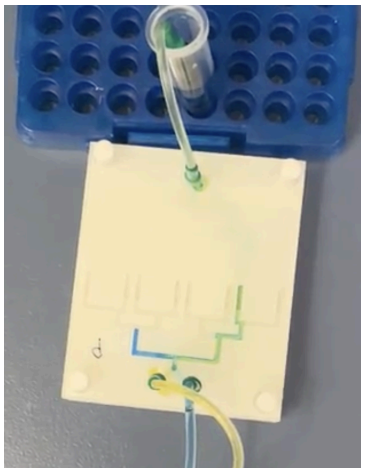	190

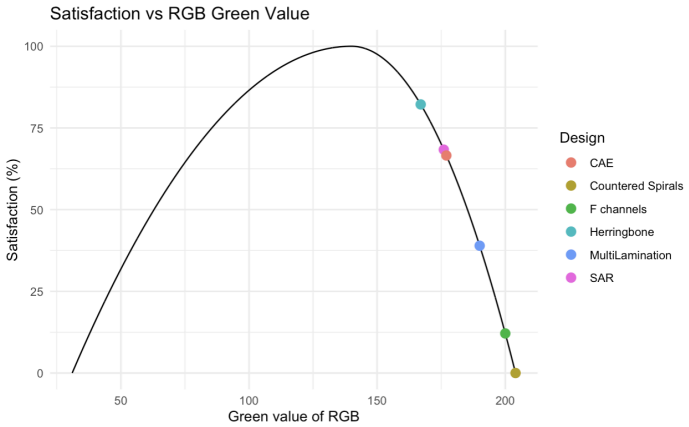

Figure 37. LPS satisfaction curves for color measurement.

4.6 Weighted Design Matrix Scoring

To rank the microfluidic chip designs based on the flow simulation results, we assigned different weights to each evaluation criterion to score our designs using a weighted design matrix:

1. Evaluation Criteria #1: Standard Deviation of Mass Fraction of Water at Output - 25%

This is our first metric for quantifying how efficient each design is at mixing through computational means. For our microfluidic chips to be functional, it must properly mix reagents to the same degree as we would manually in the lab. This criteria may also be the most variant between the designs, providing an important metric to score and rank the designs based on efficiency.

2. Evaluation Criteria #2: Time required to run flow simulations - 10%

The end users of our microfluidic chips would be our wet lab members using the chips in the lab; simulation runtime would therefore be the least of their concern. However, the simulation runtime reflects how accurate our models are which would in turn provide better and more precise chips for wet lab members to use. Furthermore, the frequency and capacity at which our hardware team can simulate the designs are also reflected by the simulation runtime.

3. Evaluation Criteria #3: Color Intensity of Titration Experiment - 30%

This is also our main metric for quantifying how efficient each design is at mixing, in reality. For our microfluidic chips to be functional, it must properly mix reagents to the same degree as we would manually in the lab. This criteria may also be the most variant between the designs, providing an important metric to score and rank the designs based on efficiency. This is weighted more than the flow simulations since these experiments are conducted on the actual microfluidic chips, providing a more accurate representation of mixing efficiency of our chips. Errors and drawbacks in the assembly and set up processes will be more apparent in these tests compared to simulations.

4. Evaluation Criteria #4: Plastic Waste - 15%

Considering that our project largely focuses on sustainability, and that the metric we use to quantify plastic waste between each design differs significantly for some designs, this is weighted higher than the simulation time. This is not weighted as the most important since ensuring mixing efficiency is still our most important need for the implementation of microfluidics.

5. Evaluation Criteria #5: Assembly Complexity - 20%

This criteria directly impacts our end users and operational team members who are assembling the chips. The difficulty of assembly would affect how well the chips are assembled,

the final set up for the wet lab members, and the mixing efficiency. Thus, this is ranked the third most important, right after the metrics that quantify how well our chips will mix.

Weight Modification for SPS Chips

Due to experiment complexity of the SPS process and reagent availability, we were unable to run the titration test experiment on the SPS chips. Thus, removing this criteria, the 30% was redistributed to the other criterias. 9% was given to the evaluation criteria #1 which corresponded to the simulation results, the only other test that tests for mixing efficiency. The rest of the 21% was distributed evenly among the other three criteria.

LPS CHIPS		***Herringbone***		***Countered Spirals***		***SAR***		***CAE***		***F-Channels***		***Multi Lamination***	
Evaluation Criteria	**Weights**	**Score / 10**	**Weighted Score**	**Score / 10**	**Weighted Score**	**Score / 10**	**Weighted Score**	**Score / 10**	**Weighted Score**	**Score / 10**	**Weighted Score**	**Score / 10**	**Weighted Score**
Standard Deviation	25%	8.684	2.171	9.99	2.4975	9.953	2.48825	9.967	2.4918	9.987	2.4968	9.98	2.495
Simulation Time	10%	9.949	0.9949	9.796	0.9796	9.796	0.9796	7.276	0.7276	9.184	0.9184	8.164	0.8164
Color Intensity	30%	8.22	2.466	0	0	6.836	2.0508	6.658	1.9974	1.211	0.3633	3.896	1.1688
Plastic Waste	15%	6	0.9	4	0.6	8	1.2	8	1.2	8	1.2	6	0.9
Assembly Complexity	20%	1.11	0.222	5.55	1.11	6.66	1.332	7.77	1.554	3.33	0.666	10	2
Total	100%		6.7539		5.1871		8.05065		7.9708		5.6445		7.3802

Figure 38. LPS Chips Weighted Design Matrix

SPS CHIPS		***Fin Baffles***		***CAE ZigZag***		***Cantor Baffles***		***Planar SAR***		***Serpentine***	
Evaluation Criteria	**Weights**	**Score / 10**	**Weighted Score**	**Score / 10**	**Weighted Score**	**Score / 10**	**Weighted Score**	**Score / 10**	**Weighted Score**	**Score / 10**	**Weighted Score**
Standard Deviation	34%	9.991	3.39694	9.963	3.38742	9.99	3.3966	9.807	3.33438	9.928	3.37552
Simulation Time	17%	9.486	1.61262	9.796	1.66532	10	1.7	9.796	1.66532	9.184	1.56128
Color Intensity	0										
Plastic Waste	22%	10	2.2	10	2.2	10	2.2	8	1.76	10	2.2
Assembly Complexity	27%	8.88	2.3976	8.88	2.3976	8.88	2.3976	6.66	1.7982	5.55	1.4985
Total	100%		9.60716		9.65034		9.6942		8.5579		8.6353

Figure 39. SPS Chips Weighted Design Matrix

5.0 Wet Lab Validation

Demonstrating the Platforms Biomanufacturing Capabilities

We were able to synthesize DNA on the platform using a hot plate and microfluidic chip. We were able to bypass the need for an expensive thermocycler, and overcame the temperature instability of a hot plate using a low cost temperature enclosure, and by providing the enzyme with adequate mixing. When tested at the same concentration as a traditional method, we got better DNA addition than benchtop LPS.

Validating the Platform as a Sustainable Alternative

We were able to produce DNA with a diluted concentration, validating our platform as a more sustainable alternative to traditional benchtop enzymatic synthesis (which was already a lot more sustainable than chemical synthesis). When tested at concentrations lower than the original benchtop workflow, we were able to get decent nucleotide addition.

References

Battat, S., Weitz, D. A., & Whitesides, G. M. (2022). An outlook on microfluidics: The promise and the challenge. *Lab on a Chip, 22*(3), 53-536. https://doi.org/10.1039/d1lc00731a

Chambers, S. (2021, Jul. 15). *Microfluidics Manufacturing: Converting Materials for Multilayer Microfluidics Devices.* Strouse. https://www.strouse.com/blog/multilayer-microfluidics-manufacturing

Channon, R. B., Menger, R. F., Wang, W., Carrão, D. B., Vallabhuneni, S., Kota, A. K., & Henry, C. S. (2021). Design and application of a self-pumping microfluidic staggered herringbone mixer. *Microfluidics and Nanofluidics, 25*(4). https://doi.org/10.1007/s10404-021-02426-x

Cortes-Quiroz, C. A., Azarbadegan, A., Moeendarbary, E. (2010). An efficient passive planar micromixer with finshaped baffles in the tee channel for wide Reynolds number flow range. *World Academy of Science, Engineering and Technology, 4,* 32-37.

Hashmi, A., & Xu, J. (2014). On the quantification of mixing in microfluidics. Journal of *Laboratory Automation, 19*(5), 488-491. https://doi.org/10.1177/2211068214540156

Hong, H. & Yeom, E. (2022). Numerical and experimental analysis of effective passive mixing via a 3D serpentine channel. *Chemical Engineering Science, 261,* 117972. https://doi.org/10.1016/j.ces.2022.117972

Husain, A., Khan, F. A., Huda, N., & Ansari, M. A. (2018). Mixing performance of split-and-recombine micromixer with offset inlets. *Microsystem Technologies : Sensors, Actuators, Systems Integration, 24*(3), 1511-1523. https://doi.org/10.1007/s00542-017-3516-4

Kim, D. S., Lee, S. H., Kwon, T. H., & Ahn, C. H. (2005). A serpentine laminating micromixer combining splitting/recombination and advection. *Lab on a Chip, 5*(7), 739-747. https://doi.org/10.1039/b418314b

Pattanayak, P., Singh, S. K., Gulati, M., Vishwas, S., Kapoor, B., Chellappan, D. K., Anand, K., Gupta, G., Jha, N. K., Gupta, P. K., Prasher, P., Dua, K., Dureja, H., Kumar, D., & Kumar, V. (2021). Microfluidic chips: Recent advances, critical strategies in design, applications and future perspectives. *Microfluidics and Nanofluidics, 25*(12), 99-99. https://doi.org/10.1007/s10404-021-02502-2

Viktorov, V., Mahmud, M. R., & Visconte, C. (2016). Numerical study of fluid mixing at different inlet flow-rate ratios in tear-drop and chain micromixers compared to a new H-C passive micromixer. *Engineering Applications of Computational Fluid Mechanics, 10*(1), 182-192. https://doi.org/10.1080/19942060.2016.1140075

Wang, X., Liu, Z., Wang, B., Cai, Y., & Song, Q. (2023). An overview on state-of-art of micromixer designs, characteristics and applications. *Analytica Chimica Acta, 1279*, 341685-341685. https://doi.org/10.1016/j.aca.2023.341685

What is Computational Fluid Dynamics (CFD)?. Ansys. https://www.ansys.com/simulation-topics/what-is-computational-fluid-dynamics#how-work

Whitesides, G. M. (2006). The origins and the future of microfluidics. *Nature (London), 442*(7101), 368-373. https://doi.org/10.1038/nature05058

Wu, Z., & Chen, X. (2019). A novel design for passive micromixer based on cantor fractal structure. Microsystem Technologies : *Sensors, Actuators, Systems Integration, 25*(3), 985-996. https://doi.org/10.1007/s00542-018-4027-7

Xia, H. M., Wan, S. Y. M., Shu, C., & Chew, Y. T. (2005). Chaotic micromixers using two-layer crossing channels to exhibit fast mixing at low reynolds numbers. *Lab on a Chip, 5*(7), 748-755. https://doi.org/10.1039/b502031j

Yin, B., Yue, W., Sohan, A. S. M. Muhtasim Fuad, Zhou, T., Qian, C., & Wan, X. (2021). Micromixer with fine-tuned mathematical spiral structures. *ACS Omega, 6*(45), 30779-30789. https://doi.org/10.1021/acsomega.1c05024